This is the accepted manuscript of the paper published in JOURNAL OF SUPERCONDUCTIVITY AND NOVEL MAGNETISM,
The published paper can be found at https://link.springer.com/article/10.1007/s10948-019-05378-0

Strain Induced Orbital Dynamics Across the Metal Insulator Transition in Thin VO_2/TiO_2 (001) Films

A. D'Elia[1,2], S.J. Rezvani[3,2], A. Cossaro[2], M. Stredansky[1], C. Grazioli[2], B. W. Li[4], C.W. Zou[4], M. Coreno[5,3], A. Marcelli[3,5,6]

[1] *Department of Physics, University of Trieste, Via A. Valerio 2, 34127 Trieste, Italy*

[2] *IOM-CNR, Laboratorio TASC, Basovizza SS-14, km 163.5, 34149 Trieste, Italy*

[3] *Istituto Nazionale di Fisica Nucleare, Laboratori Nazionali di Frascati, 00044 Frascati, Italy*

[4] *National Synchrotron Radiation Laboratory, University of Science and Technology of China, Hefei 230029, People's Republic of China*

[5] *ISM-CNR, Istituto Struttura della Materia, LD2 Unit, Basovizza Area Science Park, 34149 Trieste, Italy*

[6] *Rome International Centre for Material Science Superstripes, RICMASS, Via dei Sabelli 119A, 00185 Rome, Italy*

Abstract

VO_2 is a strongly correlated material, which undergoes a reversible metal insulator transition (MIT) coupled to a structural phase transition upon heating (T = 67 °C). Since its discovery, the nature of the insulating state has long been debated and different solid-state mechanisms have been proposed to explain its nature: Mott-Hubbard correlation, Peierls distortion, or a combination of both. Moreover, still now, there is a lack of consensus on the interplay between the different degrees of freedom: charge, lattice, orbital, and how they contribute to the MIT. In this manuscript, we will investigate across the MIT the orbital evolution induced by a tensile strain applied to thin VO_2 films. The strained films allowed to study the interplay between orbital and lattice degrees of freedom and to clarify MIT properties.

1. Introduction

The vanadium ([Ar] $3d^3 4s^2$) element is very reactive and can be synthesized in many mixed valence oxides with different oxidation states and stoichiometry, e.g., VO, V_2O_3, V_3O_5, VO_2, V_6O_{13}, V_4O_7, and V_2O_5. This class of oxides bears the seed of a strong electronic correlation and has been widely studied since the early times of X-ray spectroscopy. The electronic transport and the spectroscopic properties of V_2O_3 [1] and VO_2 [2], as well as the complex local structure of V_2O_5 [3] have always attracted interest, and still today, their investigation is a hot topic in materials science, [4–6] with many potentials for technology applications [7]. Among the vanadium oxides, VO_2 is one of the most stimulating systems. It exhibits a reversible, temperature-triggered (67 °C) metal insulator transition (MIT) coupled to a structural phase transition (SPT) from the high-temperature tetragonal metal phase to the low-temperature monoclinic insulator phase characterized also by a clear nanoscale phase separation [7–9]. Since its discovery in the late 50s [10], the nature of the VO_2 MIT has been the object of debate within the scientific community. A transition driven by the strong electron correlation, i.e., the Mott-Hubbard transition [11, 12], by the Peierls structural distortion [13–15], or by a cooperative Mott-Peierls mechanism are the most favored models for VO_2 MIT [16]. While the structurally induced effects on the electronic properties of the materials, in particular at low dimensions and high strain, are well known, [17–20] a clear correlation among lattice, orbital, and electronic degrees of freedom and MIT feature is still missing.

In this structure, each metal site is surrounded by slightly distorted oxygen octahedral and the crystal field splits the degenerate 3d manifold into 3 t_{2g} and 2 e^{σ} levels. The small orthorhombic distortion further splits the 3 t_{2g} levels in one singly degenerate a_{1g} and two e^{π} levels. According to the Goodenough model [14], V 3d and O 2p orbitals hybridize forming bonds of σ and π symmetry. Their unoccupied levels are identified as π^*(e^{π} character) and σ^* (e^{σ} character). The a_{1g} orbital is populated by unpaired 3d electrons and is called $d_{\parallel}$. The dimerization of vanadium atoms in the insulating phase splits the $d_{||}$ originating empty $d_{||}^*$ (with t_{2g} character). In the metallic phase, the $d_{||}^*$ is oriented along the c_r axis and along the V-V dimer in the insulating phase. This bond is strictly related with the unidimensional V-V dimer chain formation in the monoclinic insulating phase [21], while the π^* has an isotropic behavior within the lattice [22]. Across the MIT, the π^* and $d_{||}^*$ collapse to the Fermi level (FL) upon being both populated. This mechanism closes the band gap.

Moreover, since π^*, $d_{||}^*$ and σ^* have mostly a 3d character;changes on the electronic structure can be followed by monitoring the absorption spectroscopy intensity at the V L2,3 edges (V 2p - > 3d) [8]. Here we present the results obtained on three different single crystalline strained films of VO2/TiO2 (001) with thickness 8, 16, and 32 nm, probing simultaneously the structural and orbital contribution to the MIT using the V $L_{2,3}$ edge XANES (X-ray Absorption Near Edge Structure) spectroscopy [23], which is a good probe of strongly correlated electronic systems [24] and of strain control of functionality of quantum materials [25–28].

2. Methods

Films of VO_2 having a thickness of 8, 16, and 32 nm were deposited on a clean substrate of TiO_2 (001) by the RF plasma-assisted oxide-MBE instrument working with a base pressure better than 4×10^{-9} mbar. At the constant growth rate of 0.1 Å/s, the thickness was controlled by adjusting the deposition time in a range from

several unit cells to tens of nanometers. During the deposition process, the substrate has been kept at the temperature of 550 °C. The interfacial cross- section has been investigated with the high-resolution scanning transmission electron microscope (STEM). High angle annular dark field (HAADF) STEM images were taken on the JEM ARM200F with a probe aberration corrector, while the diffraction pattern was acquired on the JEM 2100 TEM. The complete details of the epitaxial film preparation are reported elsewhere [23, 29].

The XANES experiments have been performed at the ANCHOR end-station of the ALOISA beamline [30] at Elettra synchrotron radiation facility. Electrons were collected at normal emission by the PSP Vacuum 120-mm electron analyzer with 2D delay line detector. The photon beam was linearly polarized in the scattering plane and impinged the sample at the magic angle (35°). Measurements were performed at constant pass energy (E_p = 20 eV).

3. Results

To discern the spectral changes observed in the XANES spectra of these films, it is necessary to understand the strain-induced modification of the VO 2 crystal structure. The TiO_2 substrate has the tetragonal (rutile) lattice structure as the metallic VO_2. Most of the considerations in the next are referred to the rutile phase of VO 2 except where specified otherwise. Since the TiO_2 substrate is oriented along the (001) surface, the lattice mismatch will affect the a and b structural parameters of the vanadium oxide films. The in-plane lattice mismatch can be calculated as:

$$M = \frac{a_s - a_f}{a_f} * 100\% \quad (1)$$

where a_s and a_f are the lattice parameters of the substrate and of the sample, respectively. Between rutile TiO_2 (a = b = 4.58 Å) and bulk VO_2 ($a = b$ = 4.55 Å), the lattice mismatch M is 0.66%. Then, to match the substrate lattice during the early stage of the epitaxial growth, a VO_2 film will undergo a tensile strain, which results in the increase of both a_r and b_r and the consequent elastic compression of c_r [22, 23, 31]. Increasing the thickness of the VO_2 film, the distortions induced by the lattice of the substrate fades and the lattice constants relax to the bulk VO_2 values. For the sample analyzed in this work, the critical thickness for which the sample can be considered bulk-like is ~ 25 nm [23].

In the tetragonal unit cell, the vanadium atoms occupy the positions (0, 0, 0) and (½, ½, ½). Each vanadium atom is surrounded by oxygen octahedra with two different V-O bond lengths. Metal and oxygen atoms separated by the apical distance share the same z value along c_r. The equatorial distance that separates the vanadium atom and the four neighboring oxygen atoms is $z = z_{metal} \pm ½$ (see Fig. 1). The two apical oxygen atoms are located at ± (u, u, 0), while the four equatorial oxygen atoms are in the positions ± (±(u-½), ∓ (u-½); ½) where u = 0.3001 at 360 K [13, 32], although V-O bond lengths are influenced by strain-induced modifications in the lattice parameters. Looking at the apical distance, this is described by:

$$J_{\text{Apical}} = J_{\text{A}} = \sqrt{u^2 a_r^2 + u^2 b_r^2} = \sqrt{2u^2 a_r^2} = \sqrt{2} u a_r \tag{2}$$

and the apical V-O bond increases linearly with the a_r length. On the other hand, the equatorial bond length includes the three lattice parameters:

$$\begin{aligned} J_{\text{Equatorial}} = J_{\text{E}} &= \sqrt{\left(u-\frac{1}{2}\right)^2 a_r^2 + \left(u-\frac{1}{2}\right)^2 b_r^2 + \frac{1}{4} c_r^2} \\ &= \sqrt{2\left(u-\frac{1}{2}\right)^2 a_r^2 + \frac{1}{4} c_r^2} \end{aligned} \tag{3}$$

Combining Eqs. 2 and 3, we may recognize that J_{A} increases with the strain, while J_{E} is almost independent since the increase in a_r is compensated by the decrease of c_r [22]. Moreover, increasing the apical V-O distance, the superposition between oxygen and vanadium orbitals decreases, and as a consequence, the 3d-2p hybridization.

Actually, the π^* orbital, which points toward other vanadium atoms and is oriented toward the oxygen corners of the octahedron, is the most affected bond [22]. Moreover, the decrease of the V-O hybridization reduces the bonding- antibonding energy separation, hence the energy of π^* orbital lowers. The d^* experiences the opposite situation. The decrease of c_r increases the overlap among orbitals within the unidimensional V-V chains, shifting to high energy the $d_{||}{}^*$ orbital. Indeed, the strain increases the π^*-$d_{||}{}^*$ splitting reversing the orbital population at the FL.

In the insulating phase, the V-O hybridization is stronger and, as a consequence, the π^* and $d_{||}{}^*$ orbital are further separated, with the second appearing at higher energy respect to the former.

The V L edges XANES spectra for the metallic and insulating phase are compared in Fig. 2.

The interpretation of the L edge shape is not straightforward. However, the L_3 edge exhibits more defined features with respect to the L_2.one. In general, the L_3 and L_2 spectra differ because of the multiplet effects in the final state [33]. In this particular case, these are negligible, whereas the presence of a strong Coster-Kronig decay (V $L_2L_3M_{4,5}$) [34] severely reduce the lifetime of the excited state $2p_{1/2}{}^1 \ 3d^{n+1}$, thus broadening the XANES line shape and making hard to recognize different adjacent features. As a consequence, we will focus our attention to the L_3 edge.

The shape of the L_3 edge is not commensurate with the shape of the O K edge spectrum available in literature [35, 36] despite they should exhibit the same features as a consequence of the V3d-O2p hybridization. This can be understood taking into account other effects: in the L_3 and L_2 XANES, there is a transfer of spectral weight away from threshold (L_3 maximum intensity 518.4 eV), the apparent reduction of the spin-orbit splitting (6.4 eV from XANES spectra, 7.3 eV from XPS [37]), and the deviation from the statistic intensity ratio $I(L_3)/I(L_2) = 2$. All features can be explained considering the strong interaction between the 2p core hole (2p) and the 3d electrons in the final state. In vanadium oxides, 2p-3d interaction is of the same order of magnitude of the spin-orbit splitting, with a severe redistribution of the spectral weight of the entire spectrum [36-38]. The main shape

changes occur in the spectral region 514-518.5 eV where the π^*, $d_{||}^*$ and σ^* orbitals are present [21, 22, 39]. Precisely, $\pi^*$and $d_{||}^*$ are not distinguishable but are located in the range 514-516.5 while σ^* is centered at 518.4 eV [21]. However, in the insulating phase, when the strain increases, the π^*-$d_{||}^*$ features become more evident because of the increasing π^*-$d_{||}^*$ splitting. To highlight the changes across the MIT, the difference spectra calculated using Eq. 4 are showed in Fig. 3.

$$I_{\mathrm{ins}} - I_{\mathrm{met}} \propto uDOS_{\mathrm{ins}} - uDOS_{\mathrm{met}} \tag{4}$$

Two main contributions can be identified at ~ 515 and 517.5 eV. The high-energy contribution associated to the σ^* orbital shifts toward low photon energy due to the rearrangements of vanadium atoms within the oxygen octahedron. The low energy contribution can be assigned to the π^*-$d_{||}^*$ rearrangement going from the insulating to the metallic phase (Fig. 4). Actually, the spectral difference is dominated by the σ^* signal whose low energy-tail may probably affect the line shape of the π^*-$d_{||}^*$ feature. Nevertheless, by integrating the difference spectra in the range 512- 518.4 eV, a clear trend as a function of thickness emerges. The thickness dependence of the integrated intensity is alike what reported in [22], pointing out that the different orbital strain dynamics are qualitatively similar in agreement with the theoretical band model reported in [23] for VO2/TiO2 (001) strained and ultra-strained films.

4. Conclusion

In this work we investigated three different single crystalline strained VO_2 films deposited over a rutile TiO_2 (001) substrate. The epitaxially grown VO_2 undergoes a tensile strain, which results in the increase of a_r and b_r to match the higher lattice constant of the substrate and in the elastical reduction of c_r. These changes in the cell unit parameters affect the oxygen octahedron, which surrounds each vanadium atoms increasing the apical V-O bond length decreasing also the V 3d-O 2p hybridization. In the metallic phase of VO_2, the induced strain reduces the hybridization, upshifts the $d_{||}^*$ empty orbital, and downshifts π^*, leading to an inversion of the $d_{||}^*$ / π^* occupation at the Fermi level. In the insulating phase, the π^* and $d_{||}^*$ orbital split increased respect to the bulk case. In order to probe the dynamical model of the orbital states, we have performed XANES measurements of the V L edges probing the Auger yield (464 eV). Across the phase transition, we point out that the major changes are observed in the π^*-$d_{||}^*$ region of the spectra with the intensity increasing simultaneously to the strain. A numerical integration in the spectral region most perturbed by the MIT is in a qualitative agreement with the theoretical models and previous measurements, confirming the reliability of XANES to probe the orbital strain dynamics across the MIT. Further theoretical and experimental investigations are necessary to improve our understanding of the interplay between orbital and lattice structure in VO_2 MIT.

References

1. Bianconi, A., Natoli, C.R.: Effect of the metal-insulator transition on vanadium K-photoabsortion spectrum in V_2O_3. Solid State Commun.27(11), 1177–1179 (1978). https://doi.org/10.1016/0038-1098(78)91137-7
2. Bianconi, A.: Multiplet splitting of final-state configurations in X- ray-absorption spectrum of metal VO_2: effect of core-hole-screening, electron correlation, and metal-insulator transition. Phys. Rev. B. 26, 2741(1982). https://doi.org/10.1103/PhysRevB.26.2741
3. Stizza, S., Mancini, G., Benfatto, M., Natoli, C.R., Garcia, J., Bianconi, A.: Structure of oriented V_2O_5 gel studied by polarized X-ray-absorption spectroscopy at the vanadium K edge. Phys. Rev. B. 40, 12229 (1989). https://doi.org/10.1103/PhysRevB.40.12229
4. Lu, Q., Bishop, S.R., Lee, D., Lee, S., Bluhm, H., Tuller, H.L., Lee, H.N., Yildiz, B.: Electrochemically triggered metal–insulator transition between VO_2 and V_2O_5. Adv. Funct. Mater. 28(34), 1803024 (2018). https://doi.org/10.1002/adfm.201803024
5. Singer, A., Ramirez, J.G., Valmianski, I., Cela, D., Hua, N., Kukreja, R., Wingert, J., Kovalchuk, O., Glownia, J.M., Sikorski, M., Chollet, M., Holt, M., Schuller, I.K., Shpyrko, O.G.: Nonequilibrium phase precursors during a photoexcited insulator-to-metal transition in V_2O_3. Phys. Rev. Lett. 120, 207601 (2018). https://doi.org/10.1103/PhysRevLett.120.207601
6. Zhu, Y., Cai, Z., Chen, P., Zhang, Q., Highland, M.J., Jung, I.W., Walko, D.A., Dufresne, E.M., Jeong, J., Samant, M.G., Parkin, S.S.P., Freeland, J.W., Evans, P.G., Wen, H.: Mesoscopic structural phase progression in photo-excited VO_2 revealed by time-resolved X-ray diffraction microscopy. Sci. Rep. 6, 1 (2016). https://doi.org/ 10.1038/srep21999
7. Brahlek, M., Zhang, L., Lapano, J., Zhang, H.-T., Engel-Herbert, R., Shukla, N., Datta, S., Paik, H., Schlom, D.G.: Opportunities in vanadium-based strongly correlated electron systems. MRS Commun. 7, 27–52 (2017). https://doi.org/10.1557/mrc.2017.2
8. Marcelli, A., Coreno, M., Stredansky, M., Xu, W., Zou, C., Fan, L., Chu, W., Wei, S., Cossaro, A., Ricci, A., Bianconi, A., D'Elia, A.: Nanoscale phase separation and lattice complexity in VO_2: the metal– insulator transition investigated by XANES via auger Electron yield at the vanadium L_{23}-edge and resonant photoemission. Condens. Matter. 2(4), 38 (2017). https://doi.org/10.3390/condmat2040038
9. Gioacchino, D., Marcelli, A., Puri, A., Zou, C., Fan, L., Zeitler, U., Bianconi, A.: Metastability phenomena in VO_2 thin films. Condens. Matter. 2(1), 10 (2017). https://doi.org/10.3390/ condmat2010010
10. Morin, F.J.: Oxides which show a metal-to-insulator transition at the neel temperature. Phys. Rev. Lett. (1959). https://doi.org/10. 1103/PhysRevLett.3.34
11. Mott, N.F.: The transition to the metallic state. Philos. Mag. (1961). https://doi.org/10.1080/14786436108243318
12. Zylbersztejn, A., Mott, N.F.: Metal-insulator transition in vanadium dioxide. Phys. Rev. B. (1975). https://doi.org/10.1103/PhysRevB. 11.4383
13. Eyert, V.: The metal-insulator transitions of VO2: a band theoretical approach. Ann. der Phys. (2002). https://doi.org/10.1002/1521-3889(200210)11:9<650::AID-ANDP650>3.0.CO;2-K
14. Goodenough, J.B.: The two components of the crystallographic transition in VO_2. J. Solid State Chem. (1971). https://doi.org/10. 1016/0022-4596(71)90091-0
15. Cavalleri, A., Dekorsy, T., Chong, H.H.W., Kieffer, J.C., Schoenlein, R.W.: Evidence for a structurally-driven insulator-to-metal transition in VO_2: a view from the ultrafast timescale [2]. Phys. Rev. B - Condens. Matter Mater. Phys. (2004). https://doi. org/10.1103/PhysRevB.70.161102
16. Weber, C., O'Regan, D.D., Hine, N.D.M., Payne, M.C., Kotliar, G., Littlewood, P.B.: Vanadium dioxide: a Peierls-Mott insulator stable against disorder. Phys. Rev. Lett. (2012). https://doi.org/10.1103/ PhysRevLett.108.256402
17. Rezvani, S.J., Perali, A., Fretto, M., De Leo, N., Flammia, L., Milošević, M., Nannarone, S., Pinto, N.: Substrate-induced proximity effect in superconducting niobium nanofilms. Condens. Matter. 4(1), 4 (2018). https://doi.org/10.3390/condmat4010004
18. Pinto, N., Rezvani, S.J., Perali, A., Flammia, L., Milošević, M.V., Fretto, M., Cassiago, C., De Leo, N.: Dimensional crossover and incipient quantum size effects in superconducting niobium nanofilms. Sci. Rep. 8, 1 (2018). https://doi.org/10.1038/s41598-018-22983-6
19. Pinto, N., Rezvani, S.J., Favre, L., Berbezier, I., Fretto, M., Boarino, L.: Geometrically induced electron-electron interaction in semiconductor nanowires. Appl. Phys. Lett. (2016). https://doi.org/10.1063/ 1.4962893
20. Rezvani, S.J., Pinto, N., Enrico, E., D'Ortenzi, L., Chiodoni, A., Boarino, L.: Thermally activated tunneling

in porous silicon nanowires with embedded Si quantum dots. J. Phys. D. Appl. Phys. (2016). https://doi.org/10.1088/0022-3727/49/10/105104
21. Lee, S., Meyer, T.L., Sohn, C., Lee, D., Nichols, J., Lee, D., Seo, S.S.A., Freeland, J.W., Noh, T.W., Lee, H.N.: Electronic structure and insulating gap in epitaxial VO_2 polymorphs. APL Mater. (2015). https://doi.org/10.1063/1.4939004
22. Aetukuri, N.B., Gray, A.X., Drouard, M., Cossale, M., Gao, L., Reid, A.H., Kukreja, R., Ohldag, H., Jenkins, C.A., Arenholz, E., Roche, K.P., Dürr, H.A., Samant, M.G., Parkin, S.S.P.: Control of the metal-insulator transition in vanadium dioxide by modifying orbital occupancy. Nat. Phys. (2013). https://doi.org/10.1038/ nphys2733
23. Fan, L.L., Chen, S., Luo, Z.L., Liu, Q.H., Wu, Y.F., Song, L., Ji, D.X., Wang, P., Chu, W.S., Gao, C., Zou, C.W., Wu, Z.Y.: Strain dynamics of ultrathin VO_2 film grown on TiO_2 (001) and the associated phase transition modulation. Nano Lett. (2014). https://doi. org/10.1021/nl501480f
24. Bianconi, A. Surface X-ray absorption spectroscopy: surface EXAFS and surface XANES. Applications of Surface Science, 6(3–4), 392–418. (1980). https://doi.org/10.1016/0378-5963(80) 90024-0
25. Bianconi, A., De Santis, M., Flank, et al. Determination of the symmetry of the $3d_9L$ states by polarized Cu L_3 XAS spectra of single crystal $YBa_2Cu_3O_{\approx 6.9}$. Physica C: Superconductivity, 153, 1760–1761. (1988). https://doi.org/10.1016/0921-4534(88)90469-8
26. Agrestini, S., Di Castro, D., Sansone, M., et al.: High Tc superconductivity in a critical range of micro-strain and charge density in diborides. J. Phys. Condens. Matter. 13(50), 11689 (2001). https:// doi.org/10.1088/0953-8984/13/50/328
27. Agrestini, S., Saini, N.L., Bianconi, G., Bianconi, A.: The strain of CuO_2 lattice: the second variable for the phase diagram of cuprate perovskites. J. Phys. A Math. Gen. 36(35), 9133 (2003). https://doi. org/10.1088/0305-4470/36/35/302
28. Agrestini, S., Metallo, C., Filippi, M., et al.: Substitution of Sc for Mg in MgB_2: effects on transition temperature and Kohn anomaly. Phys. Rev. B. 70(13), 134514 (2004). https://doi.org/10.1103/ PhysRevB.70.134514
29. Fan, L.L., Chen, S., Wu, Y.F., Chen, F.H., Chu, W.S., Chen, X., Zou, C.W., Wu, Z.Y.: Growth and phase transition characteristics of pure M-phase V_{O2} epitaxial film prepared by oxide molecular beam epitaxy. Appl. Phys. Lett. (2013). https://doi.org/10.1063/1. 4823511
30. Costantini, R., Stredansky, M., Cvetko, D., Kladnik, G., Verdini, A., Sigalotti, P., Cilento, F., Salvador, F., De Luisa, A., Benedetti, D., Floreano, L., Morgante, A., Cossaro, A., Dell'Angela, M.: ANCHOR-SUNDYN: a novel endstation for time resolved spectroscopy at the ALOISA beamline. J. Electron Spectros. Relat. Phenomena. (2018). https://doi.org/10.1016/j.elspec.2018.09.005
31. Muraoka, Y., Hiroi, Z.: Metal-insulator transition of VO_2 thin films grown on TiO_2 (001) and (110) substrates. Appl. Phys. Lett. (2002). https://doi.org/10.1063/1.1446215
32. Rogers, D.B., Shannon, R.D., Sleight, A.W., Gillson, J.L.: Crystal chemistry of metal dioxides with rutile-related structures. Inorg. Chem. (1969). https://doi.org/10.1021/ic50074a029
33. de Groot, F.M.F.: Differences between L_3 and L_2 X-ray absorption spectra. Phys. B Phys. Condens. Matter. (1995). https://doi.org/10. 1016/0921-4526(94)00817-F
34. Sawatzky, G.A., Post, D.: X-ray photoelectron and Auger spectroscopy study of some vanadium oxides. Phys. Rev. B. 20, 1546–1555 (1979). https://doi.org/10.1103/PhysRevB.20.1546
35. Ruzmetov, D., Senanayake, S. D., Ramanathan, S.: X-ray absorption spectroscopy of vanadium dioxide thin films across the phase - transition boundary. Phys. Rev. B - Condens. Matter Mater. Phys. (2007). https://doi.org/10.1103/PhysRevB.75.195102
36. Abbate, M., De Groot, F.M.F., Fuggle, J.C., Ma, Y.J., Chen, C.T., Sette, F., Fujimori, A., Ueda, Y., Kosuge, K.: Soft-x-ray-absorption studies of the electronic-structure changes through the VO_2 phase transition. Phys. Rev. B. (1991). https://doi.org/10.1103/PhysRevB. 43.7263
37. Silversmit, G., Depla, D., Poelman, H., Marin, G.B., De Gryse, R.: Determination of the V2p XPS binding energies for different vanadium oxidation states (V^{5+} to V^{0+}). J. Electron Spectros. Relat. Phenomena. 135, 167–175 (2004). https://doi.org/10.1016/j. elspec.2004.03.004
38. Zaanen, J., Sawatzky, G.A., Fink, J., Speier, W., Fuggle, J.C.: $L_{2,3}$ absorption spectra of the lighter 3d transition metals. Phys. Rev. B. (1985). https://doi.org/10.1103/PhysRevB.32.4905
39. Haverkort, M.W., Hu, Z., Tanaka, A., Reichelt, W., Streltsov, S.V., Korotin, M.A., Anisimov, V.I., Hsieh, H.H.,

Lin, H.J., Chen, C.T., Khomskii, D.I., Tjeng, L.H.: Orbital-assisted metal-insulator transition in VO_2. Phys. Rev. Lett. (2005). https://doi.org/10.1103/ PhysRevLett.95.196404

Figures

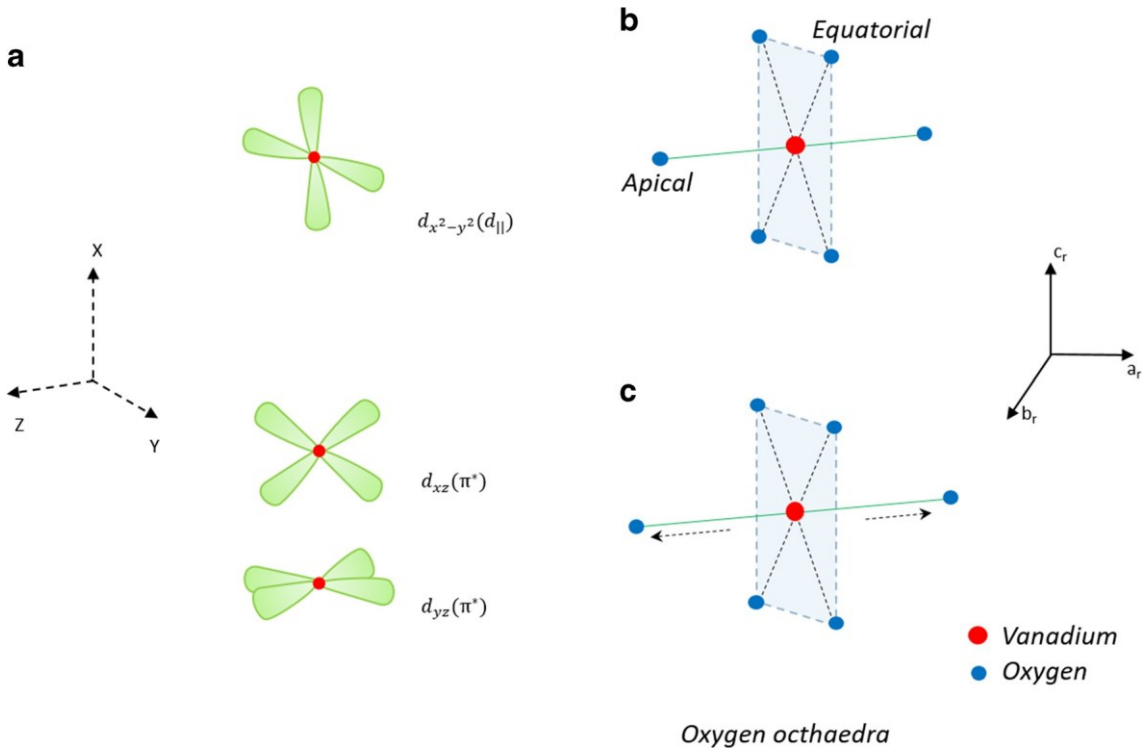

Fig. 1 a Representation of the π^* and $d_{||}{}^*$ orbitals in the octahedral frame of reference XYZ. b Oxygen octahedron surrounding V atom in the bulk case. c Schematic representation of the strain effect on the oxygen octahedron. The mismatch between TiO_2 ($a_r = b_r = 4.58$ Å) and VO_2 ($a_r = b_r = 4.55$ Å) increases the a_r and b_r lattice parameters in the epitaxial film while decreasing c_r. This results also in the increase of the apical V–O bond length. The reference frame of the octahedron is rotated by 45° respect to the tetragonal unit cell ($a_r b_r c_r$)

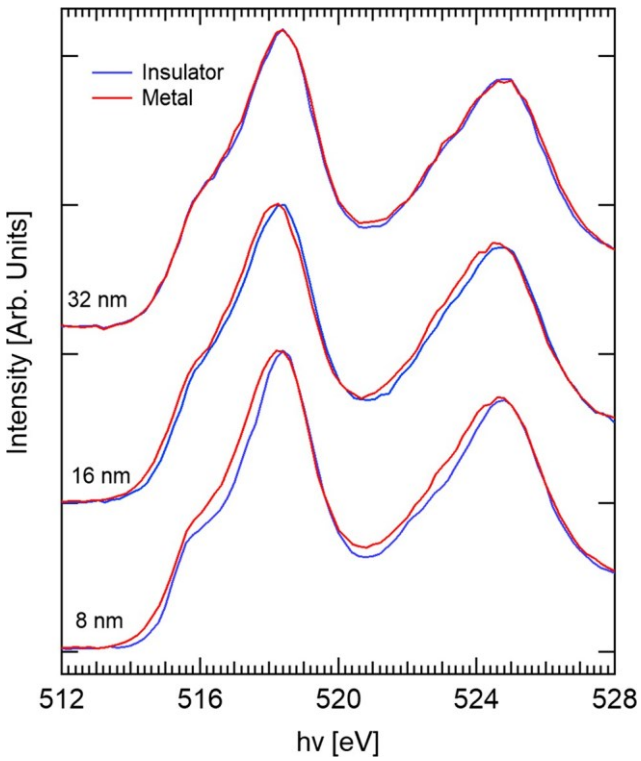

Fig. 2 Comparison among XANES spectra (Auger V $L_3M_{23}M_{45,}$ 464 eV) in the hv range (512–528 eV) of the insulating (blue line 30 °C) and metallic (red line 90 °C) phases of different VO_2 samples. From top to bottom: strained samples of 32, 16, and 8 nm. The spectra are normalized to the incident photon flux and to the L_3 maximum.

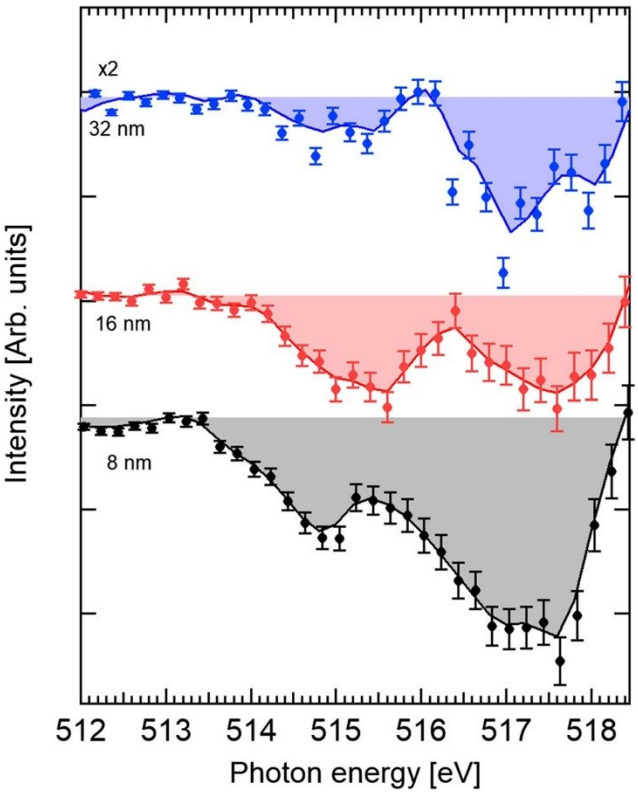

Fig. 3 Comparison among the difference of the intensity of the XANES spectra showed in Fig. 2 in the energy range 512–518.4 eV. The dots represent the experimental points, while the continuous line is the smoothed curve of the experimental points (binomial algorithm), which is used as a guide for eyes. From top to bottom: films of 32, 16, and 8 nm thickness. For sake of clarity, the spectra are vertically shifted and the difference spectrum of the 32 nm film is multiplied by 2

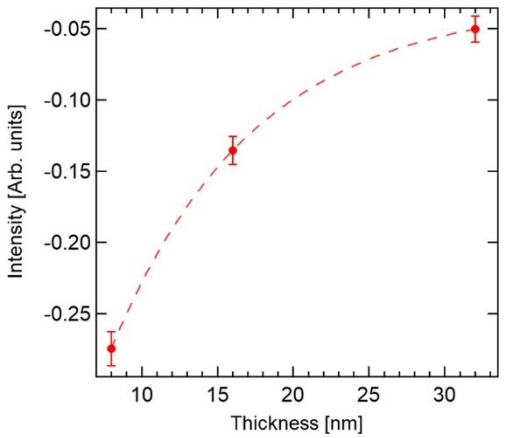

Fig. 4 The integrated differences as a function of the film thickness. The integration of the differences has been performed using a trapezoidal algorithm and in the photon energy range 512–518.4 eV. The dashed line is a guide for the eye.